

Isospin character of the “isoscalar” giant quadrupole resonance in ^{118}Sn

D. J. Horen, F. E. Bertrand, J. R. Beene, and G. R. Satchler
Oak Ridge National Laboratory, Oak Ridge, Tennessee 37831

W. Mittig, A. C. C. Villari,* Y. Schutz, Zhen Wenlong,[†] and E. Plagnol
Grand Accélérateur National d'Ions Lourds, 14021 Caen CEDEX, France

A. Gillibert
Département de Physique Nucléaire/Basse Energie, Centre de'Etudes Nucléaires de Saclay,
91191 Gif-sur-Yvette CEDEX, France
(Received 13 August 1990)

The scattering of 84-MeV/nucleon ^{17}O ions by ^{118}Sn has been studied. Inelastic cross sections for excitation of the 2.327-MeV state (3^-), the giant quadrupole resonance, and the giant monopole resonance are reproduced by distorted-wave approximation calculations using the deformed potential model and assuming isoscalar transitions. A minimum predicted in the angular distribution at $\theta_{c.m.} = 1.9^\circ$ from utilization of the small $B(E2)\uparrow$ strength suggested by π^+/π^- scattering is not apparent in the data.

I. INTRODUCTION

During the past several years, results from π^-/π^+ inelastic scattering have suggested that the “isoscalar” giant quadrupole resonance (GQR) contains a significant isovector component as evidenced by determinations of the ratio of the r^2 radial moments of the neutron and proton transition densities M_n/M_p considerably greater than N/Z .¹⁻³ This is contrary to the generally assumed “isoscalar” character of the GQR deduced from inelastic hadron scattering, as well as the isoscalar character predicted by various theoretical models (see Refs. 4 and 5, and references therein). However, Peterson and de Haro, and Castel, Boucher, and Toki have proposed that the neutron wave functions in the continuum extend beyond those for the protons and this leads to a natural explanation of the M_n/M_p enhancement observed in the π^-/π^+ measurements.⁶

Most measurements of the GQR have used probes which interact predominantly via the nuclear interaction or Coulomb interaction alone. Hence, to define M_n/M_p it has been necessary to combine results from two different probes. Such methods can sometimes lead to inaccuracies due to inconsistent analyses of the data. To circumvent such problems, we have recently investigated the determination of M_n/M_p from a single measurement in which both interactions play a significant role by using inelastic scattering of heavy ions.^{7,8} Here, one seeks a signature in the differential angular distribution which can arise from interference between the nuclear and Coulomb amplitudes for exciting the GQR. From application of this technique to excitation of the GQR in ^{208}Pb , we found that $M_n/M_p \approx N/Z$, i.e., the resonance is essentially “pure” isoscalar.

In this work, we apply the method to the case of ^{118}Sn for which the π^-/π^+ scattering suggests² $M_n/M_p = 2.38$ vs $N/Z = 1.36$.

II. EXPERIMENTAL

The experiment was performed at the Grand Accélérateur National d'Ions Lourds (GANIL), in Caen, France. We used an incident beam of 84 meV/nucleon ^{17}O ions, and detected the scattered ions with the energy loss spectrometer—Spectromètre à Perte Energie GANIL (SPEG).⁹ Particle energy and identification were accomplished by reconstruction of the trajectories of the scattered ions using two wire chambers (each of which measured an x, y position), an ion chamber, and a plastic scintillator for time of flight. The target consisted of a 95.75% ^{118}Sn self-supported foil of areal density 1.83 mg/cm². The overall experimental resolution was ~ 780 keV.

The spectrometer (SPEG) was set at an angle of 2.47° relative to the incident beam line. The nominal horizontal angular acceptance of SPEG is $\pm 2^\circ$, but the left horizontal entrance slit can be opened to 11° , and this was used as the beam stop. SPEG was tuned so that the focal plane coincided with the location of a moveable beam block which could be utilized to stop the elastic events from proceeding to the detector system when making inelastic scattering measurements. Relative angular calibrations in both θ and ϕ were made with the aid of a slotted plate. After establishing the relation between the position of the left horizontal slit and the θ calibration, the absolute scattering angle was determined to less than 0.1° by opening the left slit until the reading of the incident beam was reduced by a factor of two (i.e., $\theta \equiv 0^\circ$). This θ calibration was confirmed by the kinematic tracking of a small hydrogen impurity in the inelastic spectra.

Elastic-scattering data were obtained for ^{118}Sn (as well as for a 1.0 mg/cm² ^{112}Sn target) over an angular range $\theta_L = 0.55-4.65^\circ$ with three settings of the left horizontal entrance slit. The vertical aperture was closed down to restrict the maximum out-of-plane scattering angle (ϕ) to

$\pm 0.18^\circ$. The data were binned in 0.1° intervals for determining differential elastic cross sections. The experimental cross sections are nearly identical for the two tin targets. However, at the smallest angles, the data fall below the values for Rutherford scattering. Optical model fits (to be discussed in the next section) required that the two

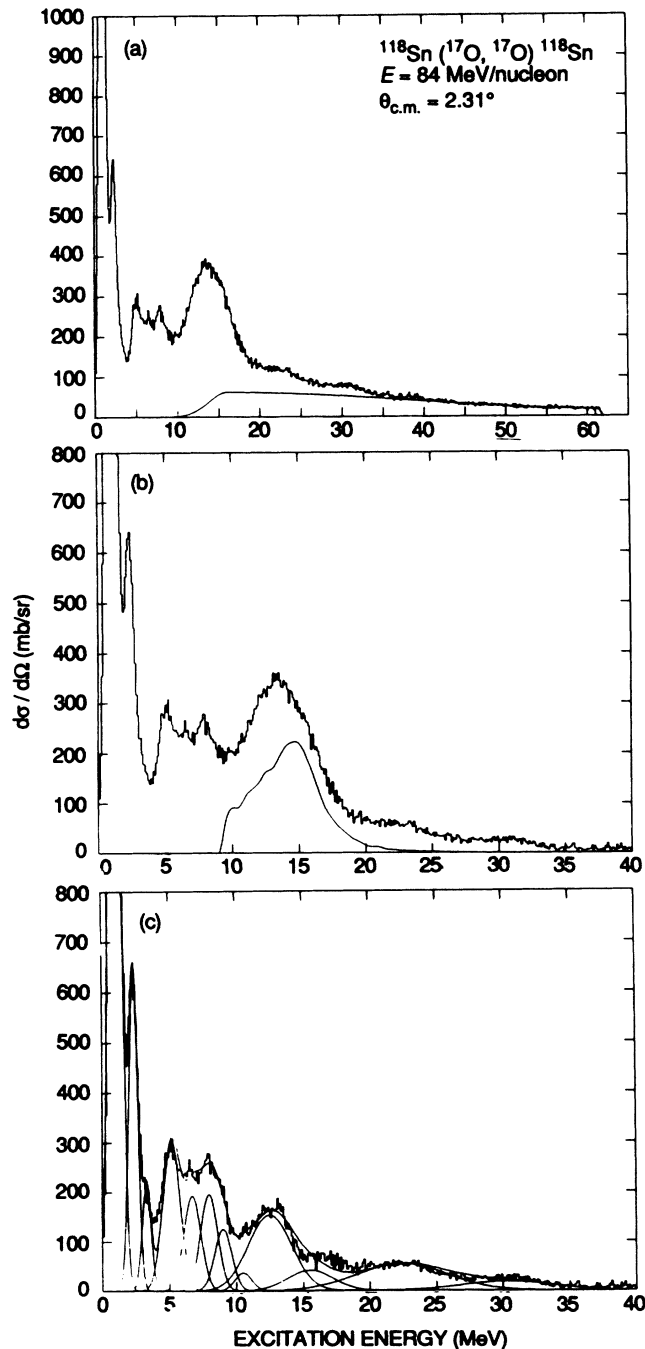


FIG. 1. Spectrum at $\theta_{c.m.} = 2.31^\circ$ from the inelastic scattering of 84 MeV/nucleon ^{17}O ions by ^{118}Sn . (a) Experimental data and solid curve depicting assumed underlying continuum. (b) Continuum subtracted spectrum and calculated GDR response function. (c) Continuum and GDR subtracted spectrum and fitted curves.

data sets be renormalized by essentially the same factor to obtain minimum χ^2 values. This renormalization factor indicates that the entrance slit did not provide a true measurement of the incident beam current.

Inelastic-scattering data were obtained with the vertical entrance slits open to accept a maximum ϕ angle of 1.3° . As noted above, elastically scattered particles were stopped at the focal plane by means of a moveable block. The inelastic data were binned in 0.1° intervals. An inelastic spectrum corresponding to $\theta_{c.m.} = 2.31^\circ$ is shown in Fig. 1(a). The large peak between 10 and 18 MeV arises mainly from the combined excitations of the giant dipole resonance (GDR) and GQR. Our procedures for decomposing the inelastic spectra are similar to those used in our studies of ^{208}Pb . There it was found that distorted-wave approximation (DWA) calculations employing only a Coulomb interaction for exciting the giant dipole resonance (GDR) reproduced the $^{208}\text{Pb}(^{17}\text{O}, ^{17}\text{O}'\gamma)^{208}\text{Pb}$ coincidence data for the GDR at an energy of 84 MeV/nucleon.⁸

III. DATA ANALYSIS AND DISCUSSION

A. Elastic scattering

Numerous searches using the computer program PTOLEMY¹⁰ were performed on the elastic-scattering data. Since the data at small angles fell below the calculated Rutherford cross section, the absolute cross section was allowed to vary in all searches. The optical model potential was assumed to be of the Woods-Saxon form

$$U(r) = -Vf(x_v) - iWf(x_w), \quad (1a)$$

with

$$f(x_i) = (1 + e^{x_i})^{-1}, \quad x_i = (r - R_i)/a_i, \quad (1b)$$

$$R_i = r_i(A_p^{1/3} + A_t^{1/3}),$$

and $i = V, W$. The Coulomb potential was assumed to be that between a point charge and a uniform charge distribution with radius $R_c = 1.20(A_p^{1/3} + A_t^{1/3})$. (Essentially identical fits were attained when a folded Coulomb potential¹⁰ between two uniform charge distributions was used.) Generally, in each search four parameters were allowed to vary, i.e., the cross-section renormalization factor, the imaginary well depth, W , the radii ($r_v = r_w$) and the diffusivities ($a_v = a_w$). In some searches, a_v and a_w were allowed to vary independently. Fixed values of V ranging between 50 and 100 MeV were used. The searches gave fits to the data of about equal quality with nearly the same cross-section renormalization factor. We finally selected the results of the fit shown in Fig. 2 attained with $V = 50.0$ MeV, $W = 43.625$ MeV, $r_v = r_w = 1.0649$ fm, and $a_v = a_w = 0.7086$ fm.

B. Inelastic scattering

1. Data reduction

The inelastic-scattering continuum was subtracted from the spectra at each angle bite. The shape of the

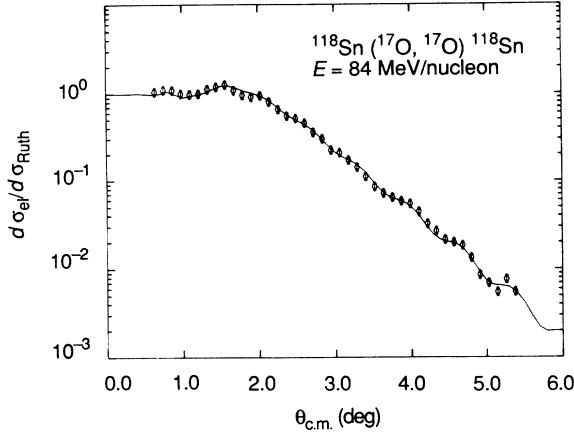


FIG. 2. Ratio of elastic-scattering cross section to Rutherford scattering vs $\theta_{c.m.}$ for 84 MeV/nucleon ^{17}O ions. The solid curve is from an optical model fit to the data (see text).

continuum was taken as a third-order polynomial above an excitation energy of 16 MeV and matched to a Gaussian peak centered at 16 MeV with an energy-dependent amplitude which tended toward zero at the neutron separation energy. A similar formulation for the continuum has been used in previous analyses of inelastic data.^{11,7,8} The polynomial was fitted to the data above $E_x = 45$ MeV. The solid line underlying the data which is plotted in Fig. 1(a) shows the shape and magnitude of the assumed underlying continuum. As can be seen in Fig. 1(a) the magnitude of the assumed continuum is small relative to that of the GR peak, and this is typical at most angles. The spectrum which results after subtraction of this continuum is shown in Fig. 1(b).

The GDR response function was calculated for each angle bin. An effective reduced $E1$ matrix element per unit energy was calculated using the photonuclear data of Fultz *et al.*¹² as

$$b(E1)\uparrow = \frac{0.09\hbar c}{16\pi^3} \sigma_\gamma(E_x)/E_x e^2 \text{ b/MeV} . \quad (2)$$

The corresponding double-differential cross section $d^2\sigma/d\Omega dE$ for $E1$ excitation was then calculated at 0.5 MeV intervals assuming only a Coulomb interaction with

TABLE I. Energies and widths of Gaussian distributions used in analysis of $^{118}\text{Sn}(^{17}\text{O}, ^{17}\text{O})^{118}\text{Sn}$ spectra.

E (MeV)	Γ (MeV)	Comment
2.327	0.780	Predominantly 3^-
3.30	0.780	
5.15	1.500	
6.70	1.500	Excitation region of LEOR
7.95	1.500	
9.00	1.500	
10.0	1.500	
12.7	3.80	GQR
15.5	4.00	GMR
22.4	8.00	
30.4	8.00	

the computer program PTOLEMY¹⁰ and the optical model potential (OMP) given above. The double-differential cross sections were integrated over the center-of-mass solid angle corresponding to each angular cut used in the data reduction in order to generate the GDR response functions. That corresponding to scattering at $\theta_{c.m.} = 2.31^\circ$ is shown in Fig. 1(b). From our earlier work⁸ on ^{208}Pb , we have confidence that the uncertainty introduced in this subtraction of the GDR strength distribution is primarily limited by that of the photonuclear data.

After subtraction of the GDR, the resulting spectrum [see Fig. 1(c)] was decomposed using a combination of Gaussian peaks whose energies and widths are listed in Table I. The peak in the spectra near 2.3 MeV was assumed to arise predominantly from excitation of the known¹³ 3^- level at 2.327 MeV. From inelastic scattering of ~ 100 -MeV alpha particles, Moss *et al.*¹⁴ reported a broad structure centered near 7 MeV with a width $\Gamma \sim 2.5$ MeV which was ascribed to a low-energy component of the isoscalar giant octupole resonance (LEOR). In our spectra, this region of excitation showed some structure which could be described by four Gaussians of equal width located at 5.15, 6.70, 7.95, and 9.00 MeV. However the relative magnitudes of the four components varied somewhat with angle. We ascribe the peak at 12.8 MeV to the excitation of the GQR. Our excitation energy of this peak is slightly below the value of 13.2 ± 0.3 MeV as reported by Youngblood *et al.*¹⁵ We have adopted the giant monopole resonance (GMR) parameters reported by these authors¹⁵ in our analysis. The other peaks listed in Table I were observed in the spectra at all angles measured, but will not be discussed further here. Differential cross sections for the peak at 2.327 (3^-), sum of the peaks at 5.15–9.0 (largely LEOR), 12.7 (GQR), and 15.5 MeV (GMR) are shown in Fig. 3. The indicated error bars on the data represent our total estimated experimental uncertainties.

2. Calculations of the differential cross sections

We have calculated the inelastic differential scattering cross sections using the deformed potential model^{16,17} and the program PTOLEMY¹⁰ in both the distorted-wave approximation (DWA) and solving the coupled channels exactly. The results of the coupled-channels calculations of the inelastic cross sections are almost identical to those obtained from the DWA calculations, which indicates that the effects of coupling on the elastic channel are negligible.

For excitation of states with $L \geq 2$, the nuclear transition potentials were taken¹⁰ as

$$H_L^N(r) = -\delta_V(L) \frac{dV(r)}{dr} - i\delta_W(L) \frac{dW(r)}{dr} , \quad (3a)$$

where $V(r)$ and $W(r)$ are obtained from the fit to elastic data. We assume the real and imaginary deformation lengths to be equal, i.e., $\delta_V(L) = \delta_W(L) = \delta(L)$, hence, Eq. (3a) reduces to

$$H_L^N(r) = -\delta_L \frac{dU(r)}{dr} . \quad (3b)$$

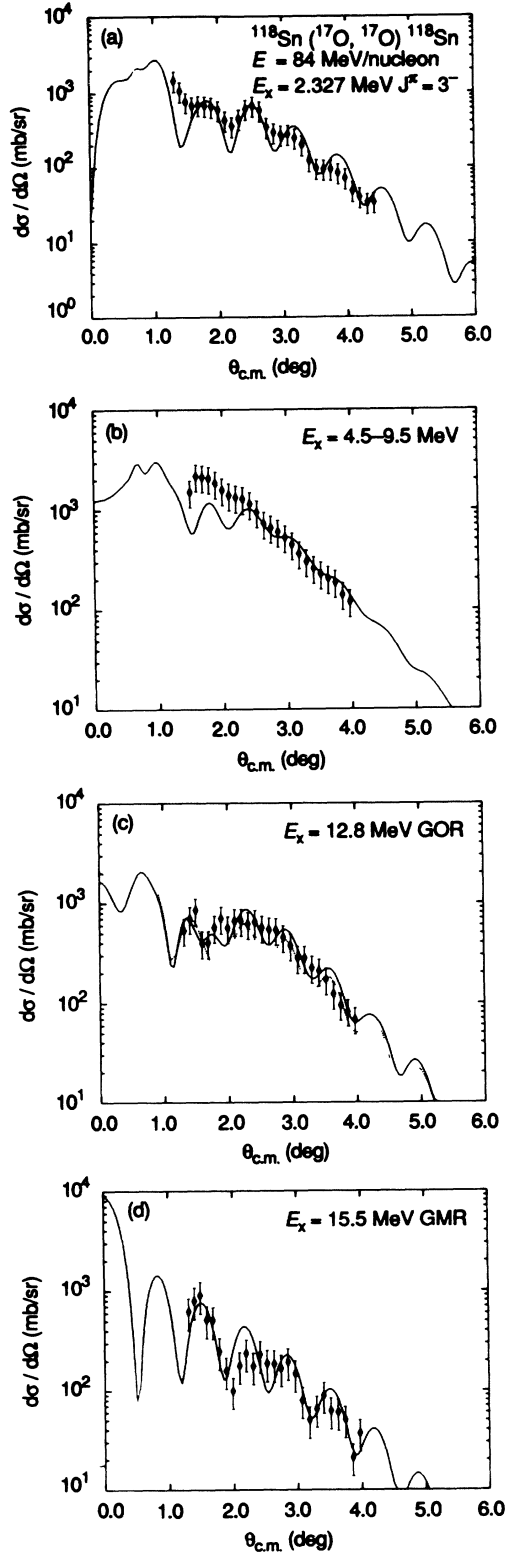


FIG. 3. Inelastic differential cross sections for the scattering of 84 MeV/nucleon ^{17}O ions by ^{118}Sn . The figures are for excitation of (a) the 2.327-MeV level, (b) the region of the LEOR (i.e., 4.5–9.5 MeV), (c) the GQR (thick solid line is from ^{17}O scattering and the thin dotted line from π^+/π^- scattering), and (d) the GMR. The curves through the data represent DWA calculations (see text).

The Coulomb interaction is taken as a multipole expansion of the potential between a point charge and an uniformly charged sphere with radius R_c , i.e.,

$$H_L^{(c)}(r) = \frac{4\pi Z_p e^2}{2L+1} [B(EL)\uparrow]^{1/2} \times \begin{cases} r^L/R_c^{2L+1} & r < R_c, \\ 1/r^{L+1} & r \geq R_c, \end{cases} \quad (4)$$

where Z_p is the atomic number of the projectile and $B(EL)\uparrow$ is given in units of $e^2 b^{2L}$.

In this model,^{16,17} the deformation length of the transition potential is assumed to equal that of the nuclear density distribution, i.e.,

$$\delta_L = \beta_L R, \quad (5)$$

where R is determined by the mean-square radius of the ground-state density distribution. Assuming a uniform distribution, a mass multipole moment can be expressed¹⁶ as

$$B(L)\uparrow = \delta_L^2 \left[\frac{3A}{4\pi} R^{L-1} \right]^2. \quad (6)$$

The mass multipole moment¹⁶ can also be given in terms of the neutron and proton moments, i.e.,

$$B(L)\uparrow = |M_n + M_p|^2, \quad (7)$$

where M_n, M_p are the r^L radial moments of the neutron, proton contributions to the transition density, respectively. Hence $B(EL)\uparrow = |M_p|^2$, and one then has

$$\left| \frac{M_n}{M_p} \right| = \left[\frac{B(L)\uparrow}{B(EL)\uparrow} \right]^{1/2} - 1. \quad (8)$$

For multipoles with $L \geq 2$, the deformation length can be expressed^{16,17} in terms of the isoscalar energy-weighted sum rule (EWSR) where the strength is localized at an energy E_x , i.e.,

$$\delta_L^2 = 2\pi\hbar^2 \frac{L(2L+1)}{3mAE_x}, \quad (9)$$

where m is the nucleon mass. Hence, from comparisons of DWA calculations with the data, one can deduce two parameters, e.g., δ_L (or M_n/M_p) and $B(EL)\uparrow$.

An analogous parameter that represents 100% of the EWSR for a monopole excitation is given by

$$\alpha_0^2 = 2\pi\hbar^2/mAE_x \langle r^2 \rangle. \quad (10)$$

Here, $\langle r^2 \rangle$ is the mean-square radius of the ground-state density distribution. For the monopole transition potential we used¹⁷

$$H_0^N(r) = -\alpha_0 \frac{c}{R_{\text{pot}}} \left[3U(r) + r \frac{dU(r)}{dr} \right], \quad (11)$$

where c is the ground-state density radius, and R_{pot} is given by Eq. (1b). We have used $c = 5.52$ fm.

C. Discussion

The calculated cross section for excitation of the 2.327-MeV level is shown as the solid curve in Fig. 3(a).

From normalization of the calculation to the data we find $B(E3)\uparrow = 0.083 \pm 0.017 e^2 b^3$. This is about 15% lower than the value $0.097 \pm 14 e^2 b^3$ reported from a Coulomb excitation measurement.¹⁸

As noted earlier, the structure in the LEOR region (≈ 4.5 – 9.5 MeV) appears to contain more than one angular momentum component. Spectra arising from excitation of the same region by inelastic alpha particles also seem to indicate that the shape of this structure changes somewhat with angle.^{14,19} The calculated curve in Fig. 3(b) represents a sum of $L=2+3$ where each multipole exhausts $\approx 18\%$ EWSR. For the LEOR, Moss *et al.*¹⁴ reported $\sim 20\%$ EWSR. Hosoyama and Torizuka found 14% $L=2$ and 39% $L=3$ in this energy interval in a study of inelastic electron scattering on ^{116}Sn .²⁰

In Fig. 3(c), we compare two calculations with the data for the GQR. The thick solid curve is for an isoscalar resonance (with $M_n/M_p = N/Z = 1.36$) which exhausts^{15,20} 60% EWSR, whereas the light dotted curve uses the π^+/π^- results, i.e., 56% EWSR with $B(E2)\uparrow = 0.0676 e^2 b^2$ which corresponds to $M_n/M_p = 2.38$. Our data do not show an indication for the marked interference minimum at $\theta_{c.m.} \approx 1.9^\circ$ as is predicted from the π^+/π^- scattering parametrization. However, they are in good agreement with the calculation which assumes a “pure” isoscalar excitation (i.e., $M_n/M_p = N/Z$) which exhausts $\sim 60\%$ EWSR and for which $B(E2)\uparrow \approx 0.181 e^2 b^2$. The $B(E2)\uparrow$ reported² for π^+/π^- scattering is more than a factor of 2.5 smaller than that for an isoscalar resonance with $M_n/M_p = N/Z$ with $\sim 60\%$ EWSR. In a recent paper, Brown *et al.*⁵ suggested that a problem may exist with the π^+ scattering results. These authors performed random-phase-approximation calculations for both a level at 2.61 MeV (2_1^+) and the GQR and their corresponding transition densities, as well as π^+ and π^- differential scattering cross sections and obtained good agreement between their π^- calculations and the π^- data, but discrepancies with the π^+ data.

The solid curve in Fig. 3(d) represents a DWA calculation using the monopole transition potential given by Eq. (11) with a strength that exhausts 125% EWSR. A similar result⁸ was found in our study of inelastic scattering of 84 MeV/nucleon ^{17}O ions by ^{208}Pb .

IV. CONCLUSIONS

We have measured the scattering of 84 MeV/nucleon ^{17}O ions by ^{118}Sn . From fits to the elastic cross sections, we have deduced optical model parameters for use in DWA and coupled-channel calculations of inelastic cross sections. The inelastic spectra were decomposed assuming an underlying nuclear continuum, a GDR response function based upon photonuclear measurements and DWA calculations, and several Gaussian-shaped peaks.

Calculations, which utilize the deformed potential model and isoscalar character for the 3^- state at 2.327 MeV, the GQR and the GMR provide a good description of the data. In particular, the GQR data do not indicate the presence of a minimum at $\theta_{c.m.} = 1.9^\circ$ as is predicted by a calculation utilizing strengths deduced from π^+/π^- scattering. The main difference between the “pure” isoscalar and the π^+/π^- parametrizations is in the magnitude of the $B(E2)\uparrow$. The value deduced from π^+/π^- scattering is approximately one-fourth that expected for a “pure” isoscalar resonance which exhausts $\sim 60\%$ EWSR.

From a recent $^{116}\text{Sn}(e, e'n)$ experiment, Miskimen *et al.* report observation of peaks at 12.2 and 17.7 MeV.²¹ They interpret the 12.2-MeV peak as arising from excitation of the GQR and deduce a $B(E2)\uparrow$ which exhausts only $37 \pm 13\%$ EWSR, whereas the 17.7-MeV peak is assigned as the GMR and exhausts $101 \pm 36\%$ EWSR. If correct, this would place their $B(E2)\uparrow$ value in reasonable agreement with that deduced from the π^+/π^- scattering for ^{118}Sn . However, these $^{116}\text{Sn}(e, e'n)$ results seem to be difficult to reconcile with those previously reported from studies of the $^{208}\text{Pb}(e, e'n)$ reaction.²² In the latter, the $(e, e'n)$ results were in excellent agreement with a $B(E2)\uparrow$ value expected for an isoscalar resonance exhausting 60% EWSR. Furthermore, theoretical calculations⁵ suggest the GQR is mainly isoscalar. On the other hand, the % EWSR for the GMR determined for ^{116}Sn and ^{208}Pb by the $(e, e'n)$ experiments are in better agreement. Although the maximum energies for neutron decay from the GQR are nearly the same for ^{116}Sn and ^{208}Pb , the availability of final states is much greater in the daughter nucleus for the former case and could lead to a much greater abundance of low-energy neutrons. Although they do not provide details, Miskimen *et al.* state that they had to correct the data for the evaporation of neutrons with energy below the threshold settings of their detectors.²¹ Obviously, these corrections would have a much greater influence on their deduced strengths in the region of the GQR than the GMR.

Finally, it should be noted that if the true character of the GQR is essentially isoscalar, and if the neutron transition density extends beyond that for the protons as has been suggested,⁶ then to attain a complete understanding of the various experimental data will require a consistent analysis, for example, comparison of folding model calculations using the same microscopic transition densities in all cases. Such an attempt is underway.

ACKNOWLEDGMENTS

This research was sponsored by the U.S. Department of Energy, under Contract No. DE-AC05-84OR21400 with Martin Marietta Energy Systems, Inc.

*Permanent address: Departamento de Física Nuclear, Instituto de Física da U.S.P., Caixa Postal 201516-01498 São Paulo, Brazil.

†Permanent address: Institute of Modern Physics (IMP), Lan-

zhou, China.

¹S. J. Seestrom-Morris, C. L. Morris, J. M. Moss, T. A. Carey, D. Drake, J. C. Douse, L. C. Bland, and G. S. Adams, *Phys. Rev. C* **33**, 1848 (1986).

- ²J. L. Ullman, P. W. F. Alons, B. L. Clausen, J. J. Kraushaar, J. H. Mitchell, R. J. Peterson, R. A. Ristinen, R. L. Boudrie, N. S. P. King, C. L. Morris, J. N. Knudson, and E. F. Gibson, *Phys. Rev. C* **35**, 1099 (1987).
- ³D. S. Oakley, M. R. Braunstein, J. J. Kraushaar, R. A. Loveman, R. J. Peterson, D. J. Rilett, and R. L. Boudrie, *Phys. Rev. C* **40**, 859 (1989).
- ⁴A. Bohr and B. Mottelson, *Nuclear Structure* (Benjamin, New York, 1969), Vol. II, Chap. 6.
- ⁵V. R. Brown, J. A. Carr, V. A. Madsen, and F. Petrovich, *Phys. Rev. C* **37**, 1537 (1988).
- ⁶R. J. Peterson and R. de Haro, *Nucl. Phys.* **A459**, 445 (1986); B. Castel, P. M. Boucher, and H. Toki, *J. Phys. G* **15**, L237 (1989).
- ⁷D. J. Horen, J. R. Beene, and F. E. Bertrand, *Phys. Rev. C* **37**, 888 (1988).
- ⁸J. R. Beene, F. E. Bertrand, D. J. Horen, R. L. Auble, B. L. Burks, J. Gomez del Campo, M. L. Halbert, R. O. Sayer, W. Mittig, Y. Schutz, J. Barrette, N. Alamanos, F. Auger, B. Fernandez, A. Gillibert, B. Haas, and J. P. Vivien, *Phys. Rev. C* **41**, 920 (1990).
- ⁹L. Bianchi, B. Fernandez, J. Gastebois, A. Gillibert, W. Mittig, and J. Barrette, *Nucl. Instrum. Methods Phys. Res.* **A276**, 509 (1989).
- ¹⁰M. H. Macfarlane and S. C. Pieper, Argonne National Laboratory Report No. ANL-76-11 (Rev. 1), 1978 (unpublished); M. Rhoades-Brown, M. H. Macfarlane, and S. C. Pieper, *Phys. Rev. C* **21**, 2417 (1980); **21**, 2436 (1980).
- ¹¹J. Lisanti, F. E. Bertrand, D. J. Horen, B. L. Burks, C. W. Glover, D. K. McDaniels, L. W. Swenson, X. Y. Chen, O. Hausser, and K. Hicks, *Phys. Rev. C* **37**, 2408 (1988).
- ¹²S. C. Fultz, B. L. Berman, J. T. Caldwell, R. L. Bramblett, and M. A. Kelly, *Phys. Rev.* **186**, 1255 (1969).
- ¹³T. Tamura, K. Miyano, and S. Ohya, *Nucl. Data Sheets* **51**, 329 (1987).
- ¹⁴J. M. Moss, D. R. Brown, D. H. Youngblood, C. M. Rozsa, and J. D. Bronson, *Phys. Rev. C* **18**, 741 (1978).
- ¹⁵D. H. Youngblood, P. Bogucki, J. D. Bronson, U. Garg, Y.-W. Lui, and C. M. Rozsa, *Phys. Rev. C* **23**, 1997 (1981).
- ¹⁶G. R. Satchler, *Direct Nuclear Reactions* (Oxford University Press, Oxford, 1983).
- ¹⁷G. R. Satchler, *Nucl. Phys.* **A472**, 215 (1987).
- ¹⁸N.-G. Jonsson, A. Backlin, J. Kantele, R. Julin, M. Luontama, and A. Passoja, *Nucl. Phys.* **A371**, 333 (1981).
- ¹⁹F. E. Bertrand, G. R. Satchler, D. J. Horen, J. R. Wu, A. D. Bacher, G. T. Emery, W. P. Jones, D. W. Miller, and A. van der Woude, *Phys. Rev. C* **22**, 1832 (1980).
- ²⁰K. Hosoyama and T. Yorizuka, *Phys. Rev. Lett.* **35**, 199 (1975).
- ²¹R. A. Miskimen, E. A. Ammons, J. D. T. Arruda-Neto, L. S. Cardman, P. L. Cole, J. R. Deininger, S. M. Dolfini, A. J. Linzey, J. B. Mandeville, B. L. Miller, P. E. Mueller, C. N. Papanicolas, A. Serdarevic, and S. E. Williamson, *Phys. Lett.* **236**, 251 (1990).
- ²²G. O. Bolme, L. S. Cardman, R. Doerfler, L. J. Koester, Jr., B. L. Miller, C. N. Papanicolas, H. Rothhaas, and S. E. Williamson, *Phys. Rev. Lett.* **61**, 1081 (1988).